Eur. Phys. J. C (2025) 85:177
https://doi.org/10.1140/epjc/s10052-025-13890-y

THE EUROPEAN PHYSICAL JOURNAL C

Regular Article - Theoretical Physics

Solutions of the Einstein–Maxwell equations with energy–momentum tensor for polytropic core and linear envelope

S. A. Mardan[1,a], **A. Khalid**[1,b], **Sana Saleem**[1,c], **Muhammad Bilal Riaz**[2,3,d]

[1] University of Management and Technology, C-II Johar Town, Lahore, Pakistan
[2] VSB-Technical University of Ostrava, IT4Innovations, Ostrava, Czech Republic
[3] Jadara University Research Center, Jadara University, Jordan

Received: 16 October 2024 / Accepted: 2 February 2025

Abstract Investigating an anisotropic charged spherically symmetric core-envelope model for dense star objects is the aim of this paper. The polytropic equation of state (EoS) defines the core of this model, while the linear EoS represents the envelope. The radiation density-containing energy–momentum tensor is used to determine the solution of the Einstein–Maxwell field equations. All three regions-core, envelope, and Reissner Nordström external metric-have perfect matching. For the intrinsic structure of the stars $SAX\ J1808.4-3658$ and $4U1608-52$, the model is physically feasible. Additionally, the Tolman–Oppenheimer–Volkoff (TOV) equation is used to verify the equilibrium state, and the adiabatic index is used to verify stability.

1 Introduction

In accordance with general relativity (GR), super-dense stars are highly dense stellar objects that drastically distort spacetime, influencing both the behavior of light and the motion of nearby objects. GR is necessary to accurately define the structure and impact of these stars because of their strong gravitational fields. Super-dense stars serve as natural laboratories for investigating nuclear matter, high-energy events, GR, and the intricate relationships between quantum mechanics and gravity. These dense objects test our understanding of physics and continue to advance scientific understanding of the cosmos and the fundamental principles governing it. In the evolution of super-dense stars, every active star eventually reaches a point where the gravitational forces are no longer able to withstand the radiation pressure from nuclear fusions in the star's core. The incidence of stellar death is implied by the moment when a star falls due to its own weight. This phenomenon is what creates dense star objects for the majority of astrophysical objects. According to Fowler [1], matter can have a dense state if it has sufficient energy to allow electrons to rotate freely within their atoms and aid in their escape. Ruderman [2] stated that super dense matter's geometry can occasionally be theoretically understood more easily than that of ordinary materials. Hwang et al. [3] tested the relative stability of strange matter compared to neutron matter.

The rare fast-spinning type of dense star $SAX\ J1808.4-3658$ is recognized as an accreting millisecond X-ray pulsar. This star was discovered in 1996 by the BeppoSAX satellite and is particularly noteworthy as the first example of a neutron star having millisecond pulsations over its X-ray emissions. The discovery of $SAX\ J1808.4-3658$ as the first accreting millisecond pulsar was announced by Wijnands and van der Klis [4]. Hufbauer [5] worked on refining giant star theory to apply to dense stars and common dwarf stars by substituting van der Waals equation for ideal gas laws. $4U1608-52$ is an X-ray binary system that consists of a low-mass neighbor star and a neutron star. We refer to this equipment as an X-ray burster. The thermonuclear eruption on the surface of the neutron star causes it to occasionally generate intense bursts of X-rays. These explosions occur when hydrogen and helium from the nearby star build up and quickly undergo nuclear fusion when they approach critical temperature and pressure. A thorough investigation of X-ray bursts from systems such as $4U1608-52$, recurrence times, adding burst characteristics, and implications for neutron star

[a] e-mail: syedalimardanazmi@yahoo.com
[b] e-mails: ayeshakhalid4238@gmail.com; S2019109012@umt.edu.pk (corresponding author)
[c] e-mail: sanasaleem@umt.edu.pk
[d] e-mails: muhammad.bilal.riaz@vsb.cz; bilalsehole@gmail.com

Published online: 12 February 2025

physics were covered by Galloway et al. [6]. The accreting millisecond X-ray pulsars $SAX\ J1808.4-3658$ were studied by Patruno and Watts [7].

Various authors have always been interested in the theoretical likelihood of taking into account self-gravitating stellar models under the influence of electric charge and electric field. Scientists can learn about the relationship between electromagnetic forces and gravitational fields in strong-field regions by studying charged stars. By shedding light on the consequences of mass and electric charge on space-time curvature, charged stars test this cohesive idea. It starts with the formation of the star from a hot, charged ionized gas. Because they are lighter, the electrons move to the star's upper surface before escaping. They were then captured by the star's surrounding electric field, which led to the star reaching a stable state with a net positive charge.Additionally, the net negative charge is formed by the interstellar gas. The Einstein–Maxwell field equations, which demonstrate the inter-dependencies between gravity and electromagnetism, unite these two forces in general relativity. The electrical energy of the charged star does not exert the gravitational pull on compact things. Actually, the star's gravitational field is supported and balanced by the energy of its charge [8]. In contrast to mass-density, Ray et al. [9] investigated the presence of charge on dense stars that take the charge dispensation. Additionally, the charge affect the star's maximum mass, radius, and stable configuration to save them from collapsing. According to Sun et al. [10], gravitational collapse occurs in compact stars when interior pressure is insufficient to counteract gravity.

The star becomes stable when the pressure gradient is balanced by the appearance of charge. In their thorough study of the effects of electric fields on stars, Takisa et al. [11] shown that charge is precisely proportional to star mass. The newly developed charged models, as explained by Maurya et al. [12], are entirely dependent on the electromagnetic field and physical characteristics (density and pressure), which vanish as the charge does. By Kumar et al. [13], charge can be viewed as the gravitational attraction counterbalanced by the Coulomb repulsion, preventing a dense object from collapsing to a point singularity. The physical viability of charge, density, pressure, and mass for a star system in class one space were examined by Maurya et al. [14]. In comparison to the uncharged situation, the repulsive force causes the mass and center density of a charged star to increase. Redshift values are also influenced by the star's charge. In a spherically symmetrical time-space, Estevez-Delgado et al. [15] demonstrated a charged star model with a regular, nonnegative, and monotonically growing charge function. Anisotropic charged stellar stars were investigated by Sharif and Gul [16] using equation of state parameters and energy bounds.

The electric field effects can be expressed algebraically under the theoretical assumption of charge-dense stars. Researchers worked on the Einstein–Maxwell field equations in order to achieve this aim. Fixing the electromagnetic field and geometric structure allows for the calculation of the precise solutions to the Einstein–Maxwell equations. While some researchers deal with static magnetovac cases, others use static electrovac cases. The electrovac case is taken into consideration when talking about electric fields, while the magnetovac case is examined when talking about magmatic fields. Harrison [17] outlined techniques for comparing the recently developed exact solutions of the Einstein–Maxwell equations to the previous field equations. Other vector-tensor field theories of charge and gravity exist in addition to the Einstein–Maxwell field theory in 4-dimensional space, as demonstrated by Horndeski [18]. Kinnersley [19] introduced the axially symmetric stationary Einstein–Maxwell field equations and their infinite-parameter symmetry group solution. Das [20] shows that the electric field is a constant multiple of the magnetic field by calculating the static Einstein–Maxwell field equation using both electric and magnetic examples. For a specific instance of the Robinson-Trautman metric, Bajer and Kowalczynski [21] obtained all of their findings from the Einstein–Maxwell equations. In the presence of strong electric fields and gravitational potentials, Komathiraj and Maharaj [22] obtained new classes of accurate findings to the Einstein–Maxwell group of equations for a dense sphere. Using a trace-free energy–momentum tensor, Lübbe and Kroon [23] assessed Einstein field equations, and the equations' findings are expressed as a general Weyl connection.

The behavior of the charge in compact stars as $PSR\ J1614-2230$, $4U\ 1608-52$, $PSR\ J1903+0327$, $EXO\ 1745-248$ and $SAX\ J1808.4-3658$ have been studied by [24]. Ratanpa et al. [25] calculated the charge for $4U\ 1820-30$, $PSR\ J1903+327$, $4U\ 1608-52$, $Vela\ X-1$, $PSR\ J1614-2230$, $Cen\ X-3$ and determined that the charge for $4U\ 1608-52$ is equal to 4.127×10^{20}. Mardan et al. [26] constructed the core-envelope model for stars such as $SAX\ J1808.4-3658$ and $4U\ 1608-52$. Prasad and Kumar [27] derived exact solutions of Einstein's-Maxwell field equation for compact stars and computed the charge for $SAX\ J1808.4-3658$ and $4U\ 1608-52$ at different points of radius. Kumar et al. [28] considered a particular form of electric field on isotropic fluid spheres. Also, give graphical analysis and numerical interpretations of model in $SAX\ J1808.4-3658$ and $4U\ 1608-52$. Ditta et al. [29] determined that charge of $SAX\ J1808.4-3658$ is 6.467×10^{18} Coulomb at radius 9.63.

Prime information on dense objects with a gravitational field can be found in the energy–momentum tensor. The energy–momentum tensor is the result of the combination of the energy densities and momentum flow. The energy–momentum tensor is often symmetric. In addition to providing numerical values for the field's energetic charac-

teristics, the energy–momentum tensor also discusses the fluid type and object motion states. Rosenfeld [30] discussed the relationship between the matter particles, gravity, and charge field and the energy–momentum tensor from any physical system. The idea of developing a new generic energy–momentum tensor that exhibits the 4-momentum and Lorentz generators comparable to conventional tensors and has finite matrix components was covered by Callan Jr. et al. [31]. Babak and Grishchuk [32] described the energy–momentum tensor by using the Lagrange function. By calculating the Euler-Lagrange form Lagrange function, Krupka [33] assessed the properties of energy–momentum tensors for the Einstein field equations. Saravi [34] shared the belief that Einstein's field equations originate from the energy–momentum tensor, which is also employed to provide physical qualities. Khrapko [35] investigated the uses and canonical significance of the energy–momentum tensor, which indicates that a gravitational field's mass-energy ratio is positive. Pimentel et al. [36] employ shear tensor, viscosity coefficients, and velocity gradients to illustrate the overall form of the energy–momentum tensor.

The core and envelope of a star are the two main components that are examined in order to have a thorough understanding of its structure. A thorough investigation is required to determine the precise distribution of the core part's constituent materials. A nuclear crust composed of baryonic matter surrounds the core portion of relativistic dense stars in numerous studies. The nature of the exotic phases of the core and envelope layers was explained by Sharma and Mukherjee [37], and the presence of charge indicates the reaction of phase change on the star. For a spherical distribution of matter, Tikekar and Jotania [38] created a two-layer model in which the fluid pressure is isotropic in the envelope and anisotropic in the core. For the core and envelop models, Takisa and Maharaj [39] solved quadratic and linear EoS, respectively, demonstrating perfect matching of the core, envelope, and exterior areas. Based on the behavior of its macroscopic properties, including the star's radius, matter type, degree of compactness, and moment of inertia, Pant et al. [40] separated the ultra dense star into two halves. Using two distinct EoS, Takisa et al. [41] investigate an uncharged anisotropic dense model, where the byronic envelope is characterized by a quadratic EoS and the quark core by a linear EoS. Every physical and structural characteristic is realistic within the core and envelope of dense stars, and continuous at the border, according to research by Gedela et al. [42]. Khunt et al. [43] created a core-envelope model for a dense object and talked about its properties and stability requirements while taking into account the anisotropic fluid in the envelope.

The EoS defines the geometrical structure of matter. Assuming that the quark that makes up a star's core is encircled by byronic matter. Given this, it is difficult to use a single EoS for the entire star and its surroundings. The stellar model's geometry calls for greater parameter involvement for this purpose, including two EoS for two different star regions and the central and envelope densities. The statement of test experiment on the investigation of EoS for dense fluid together with statistical mechanics that associate to intermolecular potential was reported by Rowlinson [44]. In order to get the best results, Angel [45] provided guidance on how to formulate the physical characteristics of EoS utilizing experimental data and diagnostic methods. The exceptional example of a polytropic EoS was the focus of Ray et al. [46], who also took into account the direct relationship between the electric charge field and star mass density. Using linear EoS applied to stars with weird quark matter, Sharma and Maharaj [47] achieved accurate solutions for anisotropic dense matter distribution and distinguished the features of computed solutions. Thirukkanesh and Maharaj [48] chose the EoS involving dark energy objects along quark matter after performing a physical examination of charged anisotropic dense spheres. In the presence of a charge field and polytropic EoS for the matter configuration, Ngubelanga and Maharaj [49] resolved the Einstein–Maxwell set of equations for anisotropic dense objects. By assuming a modified type of polytropic EoS in Korkina-Orlyanskii spacetime with a variable polytropic index, Singh et al. [50] demonstrated the anisotropic dense stars.

The charged anisotropic solution for astronomical compact matter in spherically symmetric spacetime is obtained in this publication. The relationship between the metric functions and the Einstein–Maxwell field equations, which are described by the energy–momentum tensor, is presented in Sect. 2. Additionally, There is discussion of line elements for the core, envelope, and boundary regions. Section 3 lists a few feasible physical requirements that are crucial to the acceptability of the developed compact star model. The obtained Einstein–Maxwell field equations for the core and envelope regions of stars with varying EoS are further specified in Sect. 4. The matching conditions of stars at the interface and outer surface were explained in Sect. 5. Section 6.2 provides a physical study, graphical presentation, and discussion of the developed core-envelope model. This section also provides the adiabatic index, TOV equation, energy conditions, and physical parameters for $SAX\ J1808.4-3658$ and $4U1608-52$. A succinct synopsis and conclusion are provided in the last Section 7.

2 Energy–momentum tensor and Einstein–Maxwell field equations

For the study of dense stars, the general form of a spherically symmetric line element with temporal, radial, and angular components is assumed. Schwarzschild coordinates

(t, r, θ, ϕ) are used to define the line element.

$$ds^2 = e^{\nu(r)}dt^2 - e^{\lambda(r)}dr^2 - r^2(d\theta^2 + sin^2\theta d\phi^2), \tag{1}$$

Here, $\lambda(r)$ represents the radial metric potential and $\nu(r)$ represents the temporal metric potential. The Einstein field equation discusses the spacetime curvature influenced by matter and energy and is written as

$$-8\pi(T_{ij} + E_{ij}) = G_{ij}, \tag{2}$$

also, defined by Ricci tensor R_{ij} and Ricci scalar R.

$$R_{ij} - \frac{1}{2}Rg_{ij} = G_{ij}. \tag{3}$$

Using the static spherically symmetric metric tensor, Mardan et al. [51] built mathematical models of compact stars that included the radiation factor in the energy–momentum tensor. The energy–momentum tensor, commonly known as the stress-energy tensor, is expressed as follows to represent the anisotropic pressure stress

$$T_{ij} = (\rho + p_t)u_iu_j - p_tg_{ij} + (p_r - p_t)s_is_j + q_iu_j + u_iq_j + \epsilon l_il_j, \tag{4}$$

Here, the density and pressure components are shown by ρ, (p_r, p_t). The fluid's four-velocity, radial null vector, and unit four-vector in a radial direction are u^i, l^i, and s^i. Additionally, q^i and ϵ represent radiation density and heat flux, respectively. The following requirements must be met by each element of the energy–momentum tensor

$$\begin{aligned} u^iu_i &= -1, \quad & u^iq_i &= 0, \quad & s^is_i &= 1, \\ s^iu_i &= 0, \quad & l^iu_i &= -1, \quad & l^il_i &= 0, \end{aligned} \tag{5}$$

and components in Eq. (4) are calculated from below equations

$$\begin{aligned} u^i &= \sqrt{\frac{1}{g_{ii}}}\delta^i_0, \quad & q^i &= q\sqrt{\frac{-1}{g_{ii}}}\delta^i_1, \\ l^i &= \sqrt{\frac{1}{g_{ii}}}\delta^i_0 + \sqrt{\frac{-1}{g_{ii}}}\delta^i_1, \quad & s^i &= \sqrt{\frac{-1}{g_{ii}}}\delta^i_1, \end{aligned} \tag{6}$$

with the knowledge $q = q(r)$. Following is the expression of electromagnetic energy–momentum tensor, which shows the flow of energy and momentum in field of electric charge.

$$E_{ij} = \frac{1}{4\pi}\left(F^\gamma_i F_{j\gamma} - \frac{1}{4}F^{\gamma\delta}F_{\gamma\delta}g_{ij}\right), \tag{7}$$

the electromagnetic field tensor in Eq. (7) is

$$F_{ij} = \phi_{j,i} - \phi_{i,j}, \tag{8}$$

plus

$$F^{ij}_{;j} = 4\pi J^i, \tag{9}$$

so, where J^i and ϕ_i are the 4-current and 4-potential density respectively, and defined for Eqs. (8, 9) as

$$J^i = \varsigma V^i, \qquad \phi_i = \Phi\delta^0_i, \tag{10}$$

where ς =charge density and $\Phi = \Phi(r)$. The total charge is calculated by

$$S(r) = 4\pi\int_0^r \varsigma r^2 e^{\frac{\lambda}{2}}dr. \tag{11}$$

Computing Eqs. (8) and (9), we obtain

$$\Phi'' - \left(\frac{\lambda'}{2} + \frac{\nu'}{2} - \frac{2}{r}\right)\Phi' = 4\pi\varsigma e^{\frac{\nu}{2}}e^{\lambda}, \tag{12}$$

and

$$\Phi' = \frac{S(r)e^{\frac{\nu}{2}}e^{\frac{\lambda}{2}}}{r^2}, \tag{13}$$

where

$$\varsigma = \frac{1}{4\pi r^2}(r^2S)'. \tag{14}$$

The system of Einstein–Maxwell field equations are

$$\left(\rho + \epsilon - \frac{S^2}{r^4}\right) = \left(\frac{\lambda'}{r} - \frac{1}{r^2}\right)e^{-\lambda} + \frac{1}{r^2}, \tag{15}$$

$$(p_r + \epsilon + \frac{S^2}{r^4}) = \left[\frac{\nu'e^{-\lambda}}{r} - \left(\frac{1 - e^{-\lambda}}{r^2}\right)\right], \tag{16}$$

$$\left(p_t - \frac{S^2}{r^4}\right) = \frac{e^{-\lambda}}{4}\left(2\nu'' + (\nu')^2 - \nu'\lambda' + \frac{2\nu'}{r} - \frac{2\lambda'}{r}\right), \tag{17}$$

here, anisotropic factor Δ is formulated from subtracting Eqs. (16) and (17)

$$\Delta = (p_t - p_r) = \left[\left(\frac{\nu''}{2} + \frac{(\nu')^2}{4} - \frac{\nu'\lambda'}{4} - \frac{\nu'}{2r} - \frac{\lambda'}{2r} - \frac{1}{r^2}\right) \times e^{-\lambda} + \frac{1}{r} - \epsilon\right]. \tag{18}$$

Here, the fluid's pressure anisotropy is defined by Δ. These situations determine the fluid pressure: (1) the isotropic pressure results if pressure anisotropy equals zero. (2) The existence of an anisotropic fluid is implied by the cancellation of the above instance. $p_t < p_r$ indicates an attractive fluid nature in an anisotropic fluid, while $p_t > p_r$ indicates a repulsive fluid nature [52]. It is important to note that when heat flow and radiation density are added, the matter arrangement becomes anisotropic. It is evident from the derivation that the heat flux term eventually drops to zero. Thus, it is evident from the set of Einstein–Maxwell field equations (15–18) that heat flux has very little impact on a static gravitational source. To make the model simpler, the following transformations are used

$$x = r^2, \quad Z(x) = e^{-\lambda}, \quad y = e^{\nu}, \tag{19}$$

now, set of Eqs. (15–18), becomes

$$\left(\rho+\epsilon-\frac{S^2}{x^2}\right)=\left[\frac{1}{x}-\left(\frac{Z'}{\sqrt{x}}+\frac{Z}{x}\right)\right], \tag{20}$$

$$\left(p_r+\epsilon+\frac{S^2}{x^2}\right)=\left[\left(\frac{y'}{y\sqrt{x}}+\frac{1}{x}\right)Z-\frac{1}{x}\right], \tag{21}$$

$$\left(p_t-\frac{S^2}{x^2}\right)=Z\left[\frac{2y''}{y}+\left(\frac{2}{\sqrt{x}}-\frac{y'}{y}\right)\left(\frac{y'}{y}+\frac{Z'}{Z}\right)\right], \tag{22}$$

as well as

$$\Delta=\left[\left(\frac{y''}{2y}-\frac{y'}{2y}+\left(\frac{y'}{2y}\right)^2+\frac{y'Z'}{2yZ}-\frac{y'}{2\sqrt{x}y}+\frac{Z'}{2\sqrt{x}Z}-\frac{1}{x}\right)Z+\frac{1}{\sqrt{x}}-\epsilon\right]. \tag{23}$$

In the context of stellar structure, matching criteria are crucial because they ensure that dense stars are stable and in a balanced state. These requirements are used at the surface where the star's internal and exterior sections meet. According to this model, the core layer (R_C) and envelope layer (R_E) determine the star's interior. Both (R_C) and (R_E) have spacetimes that are

$$ds^2|_C=(e^{\nu_C(r)}dt^2)-(e^{\lambda_C(r)}dr^2)-(r^2(d\theta^2+sin^2\theta d\phi^2)), \tag{24}$$

along with

$$ds^2|_E=(e^{\nu_E(r)}dt^2)-(e^{\lambda_E(r)}dr^2)-(r^2(d\theta^2+sin^2\theta d\phi^2)), \tag{25}$$

together with Eqs. (24, 25), we match the Reissner-Nordström exterior spacetime (R_B) where $r=R$.

$$ds^2|_B=\left(1-\frac{(2M)}{R_E}+\frac{Q^2}{R_E^2}\right)dt^2-\frac{dr^2}{\left(1-\frac{(2M)}{R_E}+\frac{Q^2}{R_E^2}\right)}-(r^2(d\theta^2+\sin^2\theta d\phi^2)), \tag{26}$$

here M, R and Q presents the total mass, raradius, and total charge of anisotropic charged objects, respectively.

3 Physical conditions of model

A stellar star model's physical conditions can be analyzed for a variety of purposes. These circumstances must be identified and appropriately displayed in order to demonstrate realistic behaviors, elaborate observations, and ensure that the model is applicable to actual events. Here is the conversation

- Uniform geometry: Every physical quantity must represent smooth and continuous behavior all over the star (including the center, core, and envelope region) [41].
- ρ, p_r and p_t: The elements like density and pressure components should be continuous as a function of r the core and envelope of dense objects [53].
- Mass, redshift, and compactification factor: All these expressions must represent continuity inside both regions of stars. Whether they increase or decrease with radial coordinate r, they must be positive and regular.
- Causality conditions: In astrophysical models, it is compulsory to admit that the speed of sound is less than the speed of light ($c=1$). For a model to be realistic and physically viable, the causality condition depending on pressure and density must not exceed the speed of light.
- Energy Conditions: These conditions are key rules in GR that express energy in spacetime. Moreover, observe the physical nature of stars with energy. The core and envelope of the star shall obey the energy conditions and should show continuity at the junction.
- TOV equations: To present the equilibrium state of the dense stars model, the forces (F_g, F_h, F_a) must be smooth and continuous at matching.
- Pressure of envelope at boundary defines that $p_r(R_r)$ vanishes [41].
- The metric potentials of the core must match the envelope [41].

4 The core-envelope model of Einstein–Maxwell field

The core of anisotropic stars is specified by Tolman VII [54] for metric potential $e^{-\lambda_C}$ along consideration of polytropic EoS, writhen as

$$Z=e^{-\lambda_C}=(1-(ax)+(bx^2)), \tag{27}$$

$$p_{r_C}=\alpha\rho^{1+\frac{1}{n}}, \tag{28}$$

The polytropic index, denoted by n in the equation above, is chosen to be 1. The nature of actual materials is oversimplified by the polytropic EoS, particularly when discussing the intricate structure of massive stars. The numerical solutions of gravitational field equations with polytropic EoS for static symmetric models and the finite radii case were provided by Nilsson and Uggla [55], who bound the polytropic index between 0 and 3.339. According to Spaans and Silk [56], polytropic models can also be used when there is pressure from turbulence and a magnetic field. The physical importance of polytropes and anisotropic fluid distribution in the presence of charge was explained by Azam et al. [57]. Nasim and Azam [58] discussed matter distribution using linear, polytropic, and quadratic EoS and concluded the conclusions

of the Einstein–Maxwell equation.

$$\frac{y'}{y} = \frac{P_1 + P_2 x + P_3 x^2 + \epsilon}{(1 - ax + bx^2)}, \tag{29}$$

$$y = exp^{\int \frac{P_1 + P_2 x + P_3 x^2 + \epsilon}{(1 - ax + bx^2)} dx}, \tag{30}$$

where

$$P_1 = \left[a\alpha\sqrt{x}\left(1 + \frac{1}{\sqrt{x}}\right) + a\sqrt{x} - bS^2\sqrt{x}\left(1 + \frac{2}{\sqrt{x}}\right)\right],$$

$$P_2 = \left[ab\alpha\sqrt{x}\left(1 + \frac{1}{\sqrt{x}}\right)\left(1 + \frac{2}{\sqrt{x}}\right) - b\sqrt{x} + \frac{\alpha S^2}{x^2}\left(1 + \frac{1}{r}\right)\right],$$

$$P_3 = \left[- \alpha b\sqrt{x}\left(1 + \frac{2}{\sqrt{x}}\right) + \frac{S^2}{x^{\frac{7}{2}}}(1 + \alpha S^2)\right],$$

now, by substituting $x = r^2$, Eqs. (27, 28), the Eqs. (20–23) becomes

$$\rho = ad_1 - bd_2 - \epsilon + \frac{S^2}{r^2}, \tag{31}$$

$$p_r = \alpha\rho^2, \tag{32}$$

$$p_t = h_1 + \left(\frac{h_2 + h_3 r^2 + h_4 r^4}{4(1 - ar^2 + br^4)}\right), \tag{33}$$

then

$$\Delta = p_t - p_r, \tag{34}$$

where

$$d_1 = \left[1 + \frac{1}{r}\right],$$

$$d_2 = \left[2r + r^2 + \frac{2r^2}{(1 - ar^2 + br^4)^{\frac{3}{2}}}\right],$$

$$d_3 = \left[(ar + a)\left(\alpha(S^2)' - \alpha br^2 - \frac{a\alpha}{2r} - \frac{\alpha S^2}{r^2}\right) + (br + 2b) \times(\alpha S^2 + \alpha br^4 + \alpha br^3 - \alpha(S^2)' r^2) + \frac{(S^2)'}{r} - br^3\right],$$

$$d_4 = \left[\alpha\left(\frac{(S^2)'}{r} - br - b - \frac{a}{2r^2} - \frac{S^2}{r^3}\right) - \frac{2}{r^3}\right]S^2,$$

$$h_1 = \left[\frac{d_3}{2r^2} + \frac{d_4}{2r^2} + \frac{S^2}{r^4} - \frac{a}{2r} - ab\alpha + br\right],$$

$$h_2 = [P_1^2 + P_2 + (2P_2P_3 + 2bP_2 r)r^6],$$

$$h_3 = \left[2P_1P_2 + P_1\left(\frac{1}{r^4} + \frac{2}{r^3} - \frac{2a}{r} + 2P_2\left(\frac{1}{r} - ar\right) + P_3(1 + 2r)\right)\right],$$

$$h_4 = [2P_1P_3 + P_2^2 - 2arP_3 + 2brP_1 + (P_3^2 + 2brP_3)r^4],$$

To learn more about the stability and equilibrium state of dense stars, the linear EoS is helpful. The linear EoS provides information about the structure and physical behavior of objects while simplifying the complex interactions between stellar pressure and matter density. The ultra-relativistic limitations for matter with an isotropic fluid distribution and linear EoS where pressure is insignificant were investigated by Goswami and Joshi [59]. Babichev [60] investigated hydrodynamically stable and unstable fluids and offered solutions for non-homogeneous linear EoS. Varela [61] added a description of anisotropic fluids with linear and nonlinear EoS to the analytical results using Krori and Barua's technique. A novel class of anisotropic charged spherically symmetric space-times was introduced by Ngubelanga [62], who also described the matter distribution using linear EoS. For the envelope, the same well-known Tolman VII [54] is used with linear EoS.

$$Z = e^{-\lambda_E} = 1 - ax + bx^2, \tag{35}$$

$$p_{r_E} = \alpha\rho + \beta, \tag{36}$$

where

$$\frac{y'}{y} = \frac{\sqrt{x}(P_4 + P_5 x)}{(1 - ax + bx^2)}, \tag{37}$$

$$y = exp^{\int \frac{\sqrt{x}(P_4 + P_5 x)}{(1 - ax + bx^2)} dx}, \tag{38}$$

here

$$P_4 = \left(2a + \frac{a}{\sqrt{x}} + \alpha S^2 - \beta + \frac{S^2}{x^2}\right),$$

$$P_5 = -b\left(1 + \alpha + \frac{a\alpha}{\sqrt{x}}\right).$$

Where a, b, α and β are arbitrary constants. Here, by putting $x = r^2$, Eqs. (35, 36), the Eqs. (20–23), we calculated following set of Einstein–Maxwell field equations for envelope region of stars,

$$\rho = \frac{ar^2 d_1 - br^2 d_2 - r^2\epsilon + S^2}{r^2}, , \tag{39}$$

$$p_r = \alpha\rho + \beta, \tag{40}$$

$$p_t = t_1 + \frac{t_2 + t_3 r^2}{4(1 - ax + bx^2)}, \tag{41}$$

then

$$\Delta = \Delta = p_t - p_r, \tag{42}$$

where

$$P_6 = \left[\frac{(S^2)'}{r} - \frac{br^2}{2} - \frac{S^2}{r} - \frac{a\alpha}{2} - \frac{2S^2}{r^3} - 2br^3 + (S^2)' r\right],$$

$$t_1 = \left[\frac{P_6}{2} - \frac{(a - 2br^2)}{2r} + \frac{S^2}{r^4}\right],$$

$$t_2 = [(P_4 r^4 - 2ar)P_4 + (1 - 2a + P_5 r^5 + br^4 + 4br^5)r P_5],$$

$$t_3 = \left[(2r^2P_4 + 2 - 2ar^2)P_5 + \left(rb + 4r^2b - 2a + \frac{1}{r^3} + \frac{2}{r^2}\right)P_4\right],$$

5 Matching conditions

The matching criteria specify the mathematical and physical mapping that must be followed at the borders between a star's core, envelope, and outer regions. Dense objects must remain continuous and exhibit a seamless transition under these circumstances. These are the mapping conditions for the equations (24, 25)

5.1 Interface matching conditions

The matching conditions for star interfaces map the core and envelope of stars, which have differing matter and pressure.

$$e^{\nu_C}(R_C) = e^{\nu_E}(R_C), \tag{43}$$
$$e^{\lambda_C}(R_C) = e^{\lambda_E}(R_C), \tag{44}$$
$$p_{r_C}(R_C) = p_{r_E}(R_C). \tag{45}$$

5.2 Mapping conditions of envelope to Reissner–Nordström space-time

The conditions presenting the mapping of envelope region of star from Eq. (25) to exterior region of star Eq. (26).

$$e^{\nu_E}(R_E) = \left(1 - \frac{2M}{r} + \frac{Q^2}{r^2}\right), \tag{46}$$
$$e^{\lambda_E}(R_E) = \left(1 - \frac{2M}{r} + \frac{Q^2}{r^2}\right)^{-1}, \tag{47}$$
$$p_{r_E}(R_E) = 0. \tag{48}$$

The constants involved in Eqs. (43–48) are stated as

$$M = \frac{1}{2}R_E^2(a - bR_E^2), \tag{49}$$
$$R_E = \frac{\sqrt{\frac{3aAb+4\pi(\sqrt{b^2(4AC+B^2)}+bB)}{Ab^2}}}{\sqrt{5}}, \tag{50}$$

where

$$C = \frac{(3a - 5bR_E^2)(3aA - 5AbR_E^2 + 8\pi B)}{64\pi^2},$$
$$\beta = \frac{(3a - 5bR_C^2)(8\pi\alpha + 5Ab(R_C^2 - R_E^2))}{64\pi^2} + \sigma,$$
$$\sigma = \frac{5bC(R_C^2 - R_E^2)}{3a - 5bR_E^2}.$$

The values of the above constants are appropriate for all physical parameters of dense objects to ensure proper behavior.

6 Physical analysis

This section examines the physical study of dense stars $SAX\ J1808.4 - 3658$ and $4U1608 - 52$. Here, the characteristics of objects are examined through the use of several physical theories and observational methods. An outline of the essential elements that make up the physical examination of stars is provided:

6.1 Geometry free from singularity

The spacetime metric's components, the metric potentials $(e^{\nu}, e^{-\lambda})$, calculate the stars $SAX\ J1808.4 - 3658$ and $4U1608 - 52$'s radial coordinates, distances, and times. $e^{-\lambda}$ must equal 1 at the center of the star and e^{ν} must not be negative. The center of these metric potential components is singularity-free, and the matching is smoothly continuous.

6.2 Physical parameters

6.2.1 Density and pressure directions

The density, tangential pressure, and radial pressure are necessary physical parameters that characterize the internal makeup of stars in a stellar model. These characteristics are continuous and correspond smoothly at the boundary with positive values throughout the dense objects, as demonstrated by Ivanov [63] (see Figs. 1, 2, 3). According to Zeldovich's criterion [47], the density to pressure ratio cannot be greater than the speed of light since doing so would have a detrimental effect on gravitational mass and result in nonphysical super-luminal speeds. In Fig. 4, it is evident that the ratios $\frac{p_r}{\rho}$ and $\frac{p_t}{\rho}$ are less than $c = 1$, therefore satisfying condition [53].

6.2.2 Anisotropy factor

The anisotropy factor calculated by subtracting p_r from p_t is continuous and shown in Fig. 5.

6.2.3 Redshift, mass–radius ratio, compactification factor and electric charge

Earman [64] derived the redshift as a test of GR and give its theoretical description. The relationship of mass is given as

$$m(x) = 4\pi \int_0^x \rho x dr, \tag{51}$$

the compactification factor defined with mass function is stated as

$$u(x) = \left[\frac{m(x)}{\sqrt{x}}\right]. \tag{52}$$

and red-shift is in the form

$$z(x) = \left[\left(\frac{1}{\sqrt{1-2u(x)}}\right) - 1\right]. \tag{53}$$

Figures 6 and 8 plot the mass and redshift. For the core area and envelope of compact stars $SAX\ J1808.4-3658$ and $4U1608-52$, the mass m and gravitational red-shift z are regular and continuous at the interface, and they begin to increase with radial coordinate r. Additionally, the compactification function u for the participating stars increases in nature with respect to r and is positively continuous at the interface.It is evident from Fig. 7 that the compactification factor falls within the bounds of Buchdahl [65].

The impact of charge and maximum measure of the charge in compact stars have been analyzed by Ray et al. [9]. They stated that a huge charge of 10^{20} Coulombs is available in compact stars. The charge for the current model is numerically calculated and listed in Table 3 for compact stars.To find the amount of charge in Coulomb, the factor 1.1659×10^{20} has to multiply in every value of Table 3. Böhmer and Harko [66] proved that for charged compact spheres there exist a limit for the ratio of mass-radius which means $Q < M$. Also, presented the lower and upper limits equations of mass-radius ratio for the charged compact star model with $Q < M$ as following.

$$\frac{Q^2}{R^2}\left(\frac{18R^2+Q^2}{12R^2+Q^2}\right) \leq \frac{2M}{R}. \tag{54}$$

$$\sqrt{M} \leq \frac{\sqrt{R}}{3} + \sqrt{\frac{R^2+3Q^2}{9R}}. \tag{55}$$

Dayanandan et al. [67] calculated the charge for compact stars at different points and satisfies Böhmer and Harko mass-radius ratio. Following these conditions, model shows that numerical solutions are consistent with the observational constraints.

6.2.4 Causality conditions

Causality conditions for accurate modeling of dense stars in stellar stars are assessed. This facilitates informational transmission in a way that is compatible with physical devices. Figure 9's $v_{sr}^2 = dp_r/d\rho$ perfectly matches the outside and meets causality requirements.

6.2.5 Adiabatic index

When evaluating the fluid type and stability of dense stars, the adiabatic index Γ is crucial. Usually, this test shows how radial pressure responds to variations in density. The adiabatic relation provided by [68] is shown below.

$$\Gamma_r = \frac{\rho + p_r}{p_r}\frac{\partial p_r}{\partial \rho}. \tag{56}$$

The Γ for stable Newtonian sphere must be greater then $4/3$ [69–71]. For both stars $SAX\ J1808.4-3658$ and $4U1608-52$, the adiabatic index is shown in Fig. 10.

6.2.6 Energy conditions

To avoid the emergence of nonphysical scenarios, model should satisfy required energy conditions to make certain that physical theories are consistently match with observed data. The energy conditions certifies that results of Einstein–Maxwell field equations are physically acceptable and stable.

(i) Null energy condition (NEC)

$$\rho + p_r \geq 0, \tag{57}$$

defines the density and radial pressure relation where energy density must be positive.

(ii) Weak energy conditions for radial and tangential pressures (WEC_r, WEC_t)

$$\rho + p_r \geq 0, \rho \geq 0, \tag{58}$$

$$\rho + p_t + \frac{E^2}{4\pi} \geq 0, \rho \geq 0, \tag{59}$$

discuss the pressures and density for model's stability and study of matter in spacetime.

(iii) Strong energy condition (SEC)

$$\rho + p_r + 2p_t + \frac{E^2}{4\pi} \geq 0, \tag{60}$$

Combines density and pressure stresses, to show strong points that support the non-repulsive behavior of gravity and presents singularity free model(see Fig. 11). In above equations $E = \frac{S}{r^2}$.

6.3 TOV equation of core-envelope model

Oppenheimer and Volkoff [72] found that a neutron star can withstand gravitational collapse up to a certain mass. Once this range is exceeded, the astrophysical body will collapse to become a black hole because no equilibrium solution can satisfy the TOV equation. Therefore, checking the equilibrium state ensures that the system is stable and within its mass limit. We deal with the TOV expression in stellar systems, which is determined by three force components. Anisotropic force (F_a), hydrostatic force (F_h), and gravitational force (F_g) are related in the TOV equation. Additionally, the sum of these forces ought to equal zero. The TOV formula given by [73].

$$\underbrace{-\frac{M_g(r)(\rho+p_r)}{r^2}e^{\frac{\nu-\lambda}{2}}}_{F_g} \underbrace{-\frac{dp_r}{dr}}_{F_h} + \underbrace{\frac{2\Delta(r)}{r}}_{F_a} = 0, \tag{61}$$

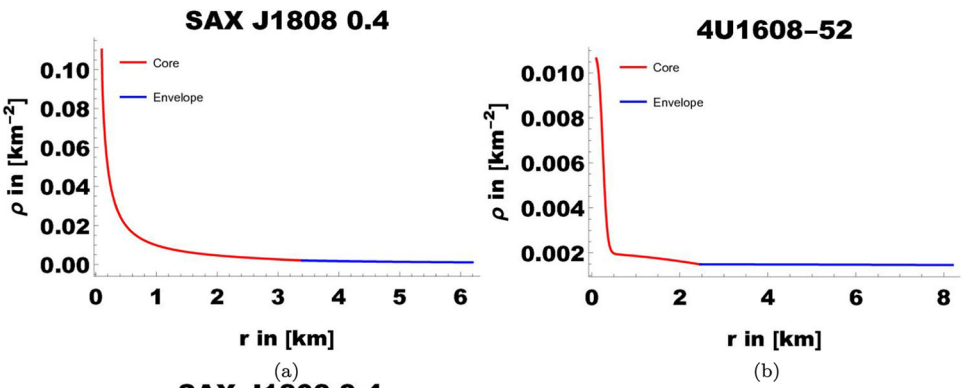

(a) (b)

Fig. 1 Nature of matter density respecting coordinate r for both dense stars

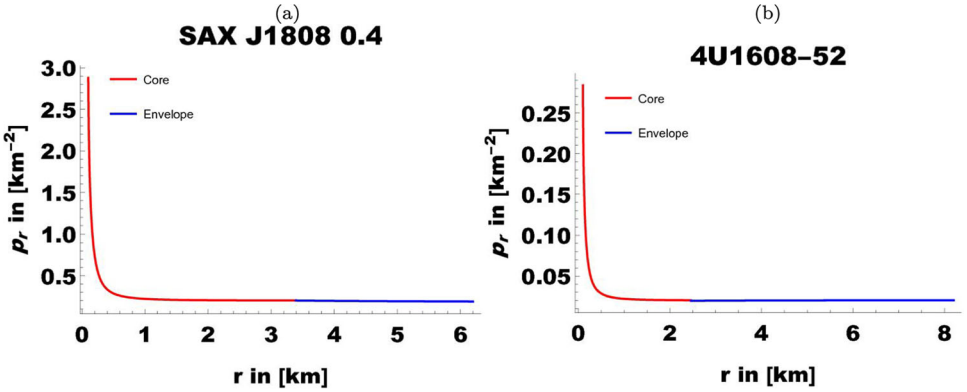

(a) (b)

Fig. 2 Nature of radial pressure respecting coordinate r for both dense stars

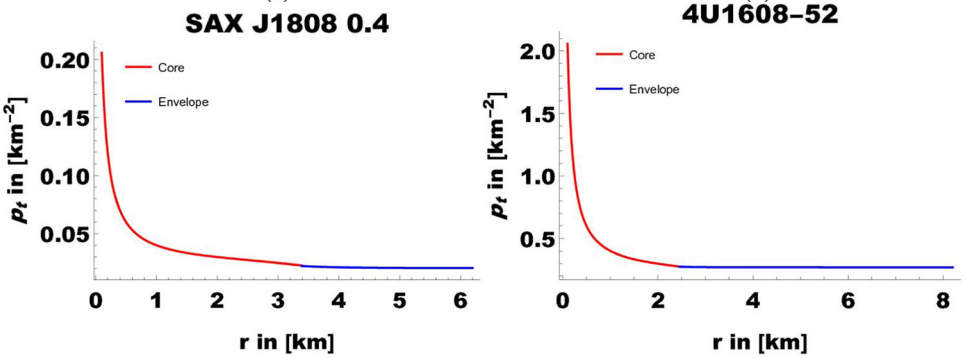

(a) (b)

Fig. 3 Nature of tangential pressure respecting coordinate r for both dense stars

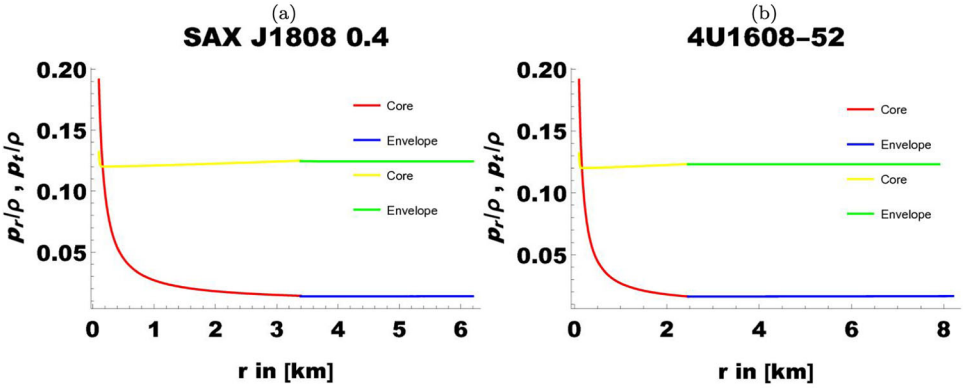

(a) (b)

Fig. 4 Nature of pressure-density relation respecting coordinate r for both dense stars

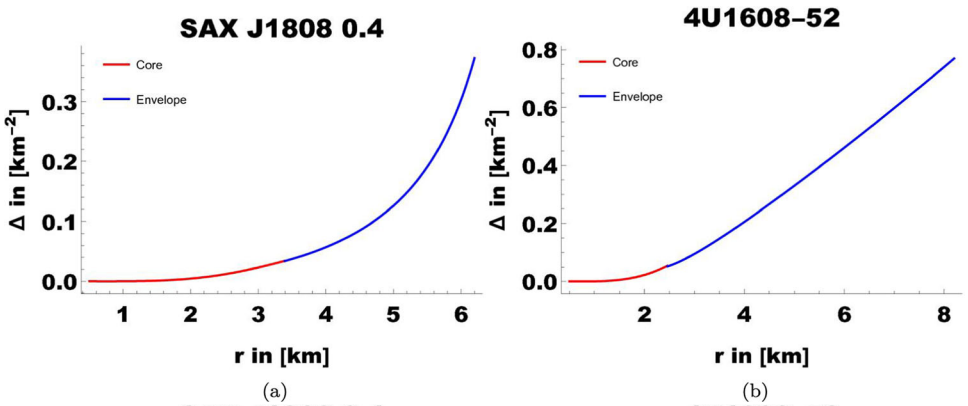

(a) (b)

Fig. 5 Nature of anisotropy equation respecting coordinate r for both dense stars

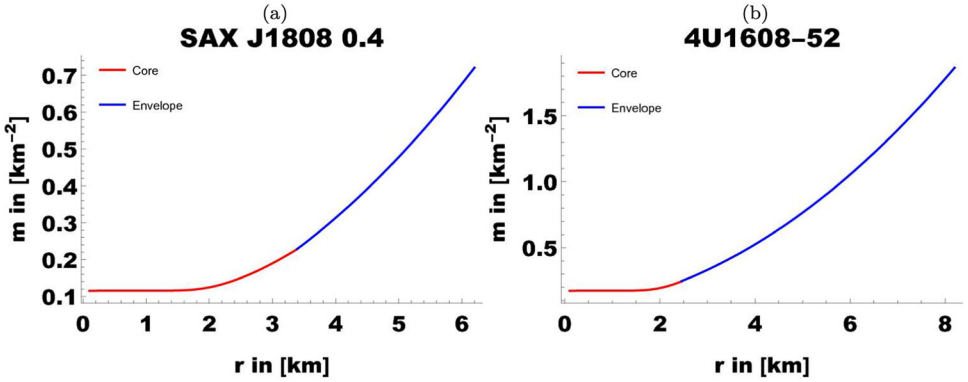

(a) (b)

Fig. 6 Nature of mass equation respecting coordinate r for both dense stars

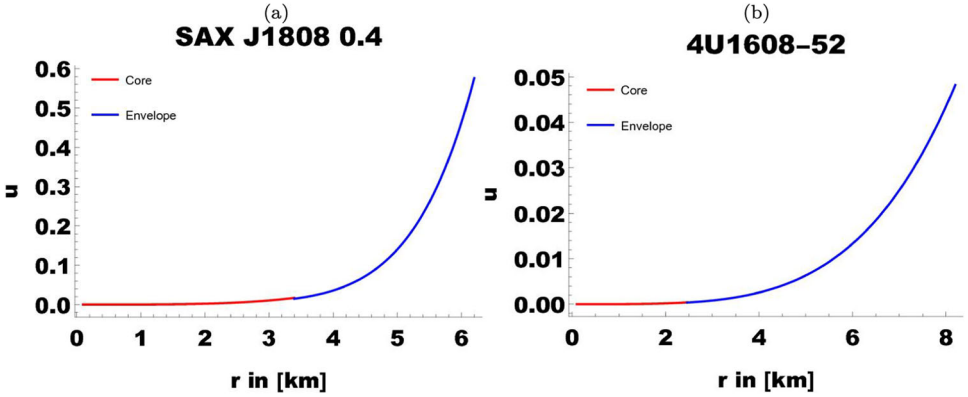

(a) (b)

Fig. 7 Nature of compactification respecting coordinate r for both dense stars

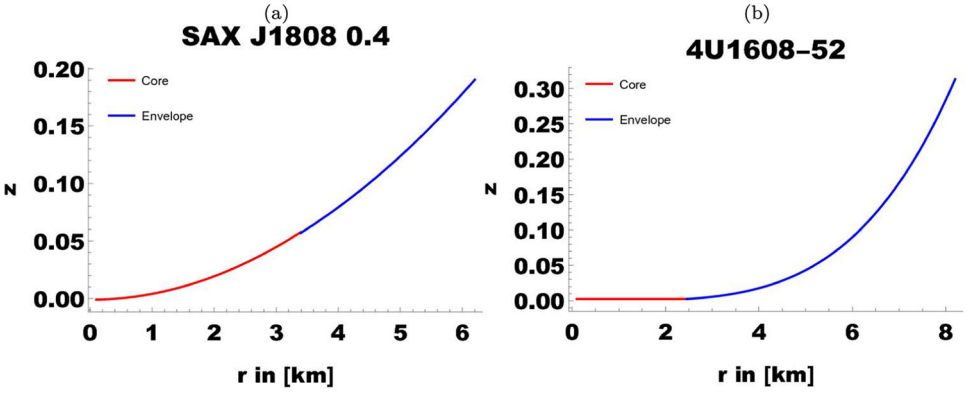

(a) (b)

Fig. 8 Nature of red-shift respecting coordinate r for both dense stars

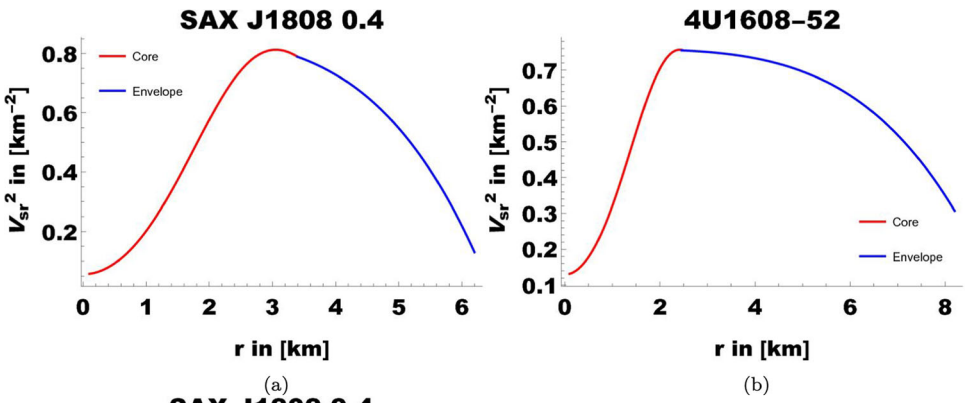

(a) (b)

Fig. 9 Nature of radial sound speed velocity respecting coordinate r for both dense stars

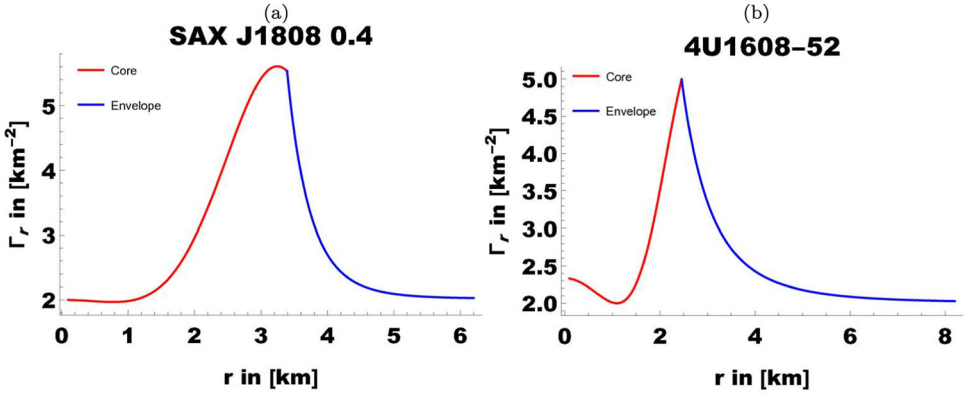

(a) (b)

Fig. 10 Nature of adiabatic index respecting coordinate r for both dense stars

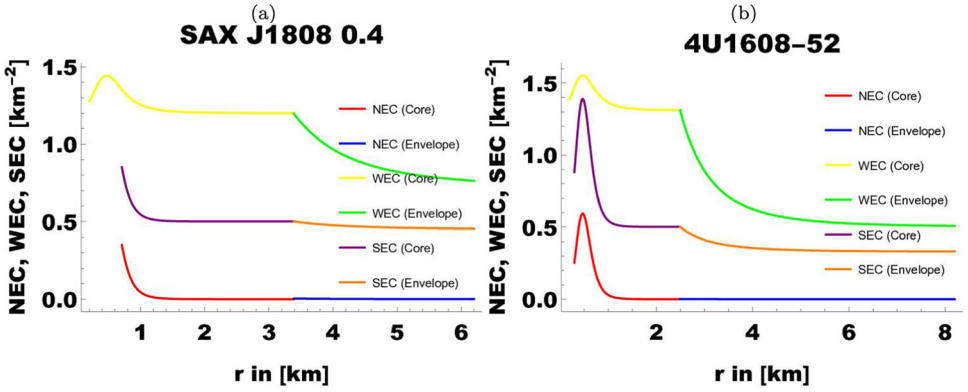

(a) (b)

Fig. 11 Nature of energy conditions respecting coordinate r for both dense stars

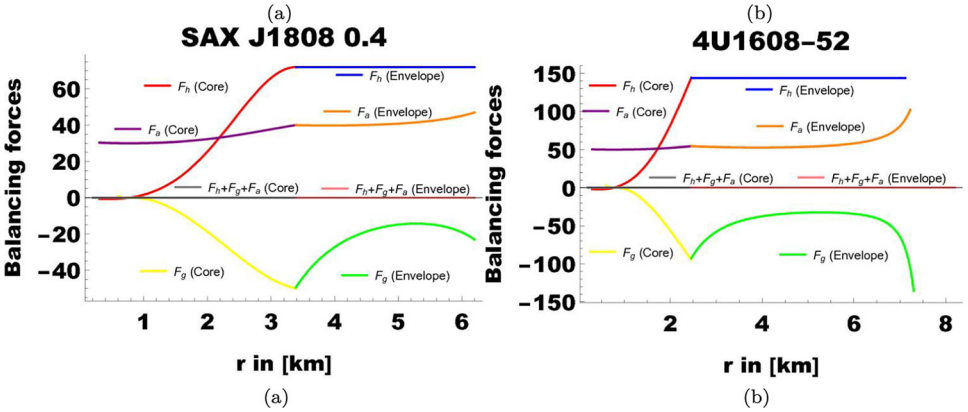

(a) (b)

Fig. 12 Nature of TOV equations respecting coordinate r for both dense stars

Table 1 Constant values for realistic star $SAX\ J1808.4-3658$

Physical Parameters	$A(\text{km})^{-2}$	$b(\text{km})^{-2}$	$B(\text{km})^{-2}$	$\beta(\text{km})^{-2}$	$R_C(\text{km})$	$M(M_\odot)$	$R_E(\text{km})$
Density (ρ)	9990	47.01	0.004	0.0001	3.393	0.7	6.2
Radial pressure (p_r)	-9991	0.01	0.05	0.001	3.393	0.7	6.2
Tangential pressure (p_t)	0.22	830	0.0032	0.1	3.393	0.7	6.2
Mass (m)	0.0022	0.1	990	0.01	3.393	0.7	6.2
Red-shift (z)	0.0022	5.1	989	0.001	3.393	0.7	6.2
Comactification factor (u)	0.00212	4.9	988	0.001	3.393	0.7	6.2
Anisotropy (Δ)	0.023	0.001	499	0.1	3.393	0.7	6.2
Radial velocity (v_{sr})	0.0032	0.006	0.0007	0.0001	3.393	0.7	6.2
Adiabatic index (Γ)	−0.0022	0.001	199	0.0012	3.393	0.7	6.2

Table 2 Constant Values for realistic star $4U1608-52$

Physical Parameters	$A(\text{km})^{-2}$	$b(\text{km})^{-2}$	$B(\text{km})^{-2}$	$\beta(\text{km})^{-2}$	$R_C(\text{km})$	$M(M_\odot)$	$R_E(\text{km})$
Density (ρ)	8.0012	20.2	0.006	0.1	2.459	1.85	8.2
Radial pressure (p_r)	-9990	0.01	0.04	0.01	2.459	1.85	8.2
Tangential pressure (p_t)	0.22	830.02	−0.00032	0.1	2.459	1.85	8.2
Mass (m)	0.0022	0.1	992	0.0012	2.459	1.85	8.2
Red-shift (z)	0.0024	0.12	991	0.011	2.459	1.85	8.2
Comactification factor (u)	0.0021	0.09	988	0.001	2.459	1.85	8.2
Anisotropy (Δ)	0.022	0.0001	290	0.002	0.1	1.85	1.85
Radial velocity (v_{sr})	0.0002	0.015	0.0001	0.001	2.459	1.85	8.2
Adiabatic index (Γ)	−0.0022	0.01	196	0.01	2.459	1.85	8.2

where gravitational mass is symbolized as $M_g(r)$ and stated as

$$M_g(r) = \frac{1}{2} r^2 \nu' e^{\frac{\nu-\lambda}{2}}, \tag{62}$$

according, Eq. (60) also be written as

$$F_g + F_h + F_a = 0. \tag{63}$$

Static and spherically symmetric configurations are taken into account while computing the TOV equation from the Einstein field equations. The TOV equation is necessary to apply GR to physical systems, such as compact stars, even if the Einstein field equations provide the theoretical foundation. According to Lattimer and Prakash [74], the TOV equation translates the spacetime curvature into useful relations, such as determining the maximum stable mass and the mass-radius ratio. Figure 12 illustrates the TOV equation's physical nature.

7 Summary and conclusion

In summary, we investigated an anisotropic core-envelope model of charged dense stars, represented by the numbers $SAX\ J1808.4-3658$ and $4U1608-52$. In the model, we set up the envelope as linear EoS and the center as polytropic EoS. The energy–momentum tensor calculated the Einstein–Maxwell field equations' results. In the current model, graphs are used to illustrate the physical nature of the parameters. Figures demonstrate the positive and continuous nature of physical quantities and metric potentials. Furthermore, we provide a list of appropriate constant values that meet the graphical behavior of objects in Tables 1 and 2.

- Figs. 1, 2 and 3 indicates that the density outline and pressure elements are positive for both stars. These parameters smoothly match at junction and are continuous.
- Fig. 4 describes regular and smooth matching behavior of pressure-density relation everywhere within the stars.
- Fig. 5 is plotted for anisotropy factor having minimum value at the center.
- Figs. 6, 7 and 8 shows regular and continuous behavior. Where compactification factor u is formulated from $\frac{M}{R}$ relation.
- Fig. 9 is a decreasing graph of radial sound speed along coordinate r satisfying the casualty condition.
- Fig. 10 is plotted according to $\Gamma > \frac{4}{3}$. It is positive, uniformly decreasing and proves stability of our model.

Table 3 The numerical values of electric charge for compact stars

r/R	$SAX\ J1808.4-3658$	$4U1608-52$
0.0	0.0000	0.0000
0.1	0.00873863	0.00348667
0.2	0.0396347	0.0711144
0.3	0.0924219	0.18387
0.4	0.167114	0.346147
0.5	0.263714	0.558139
0.6	0.382222	0.819893
0.7	0.522638	1.13143
0.8	0.684962	1.49275
0.9	0.869195	1.90386
1.0	1.07533	2.36477

- Fig. 11 of energy conditions evident that core and envelope must satisfy energy requirements for considered stars.
- Fig. 12 of TOV equation plot all 3 forces and their addition. Which concludes that our model of stars is in state of balanced equilibrium.
- The dense star $SAX\ J1808.4-3658$ with mass $M(M_{\odot}) = 0.7$, radius $R_C(\text{km}) = 3.393$, $R_E(\text{km})(\text{km}) = 6.2$ and $\alpha(\text{km})^{-2}(\text{km})(\text{km}) = 1.22$.
- The dense star $4U1608-52$ with mass $M(M_{\odot}) = 1.85$, radius $R_C(\text{km}) = 2.459$, $R_E(\text{km}) = 8.2$ and $\alpha(\text{km})^{-2} = 0.050$.
- Table 3 shows numerical values of charge on $SAX\ J1808.4-3658$ where $a = 1.2$, $b = 0.00002$ and $\alpha = 54$.
- For $4U1608-52$ values of charge are listed in Table 3 with computed by parametric values $a = 6.2$, $b = 0.000032$ and $\alpha = 19.4$.

Acknowledgements This article has been produced with the financial support of the European Union under the REFRESH-Research Excellence For Region Sustainability and High-tech Industries project number CZ.10.03.01/00/22_003/0000048 via the Operational Programmed Just Transition.

Data Availability Statement This manuscript has no associated data. [Authors' comment: This is theoretical study so, no data will be deposited.]

Code Availability Statement The manuscript has no associated code/software. [Author's comment: This is theoretical study so, no code will be provided.]

Funded by SCOAP[3].

References

1. R.H. Fowler, On dense matter. Mon. Not. R. Astron. Soc. **87**, 114 (1926)
2. M. Ruderman, Superdense matter in stars. J. Phys. Colloq. **30**, 152 (1969)
3. W.Y.P. Hwang, C. Liu, K.C. Tzeng, Dense stars with exotic configurations. Z. Phys. A **338**, 223 (1991)
4. R. Wijnands, M. van der Klis, A millisecond pulsar in an X-ray binary system. Nature **394**, 344 (1998)
5. K. Hufbauer, Stellar structure and evolution, 1924–1939. J. Hist. Astron. **37**, 203 (2006)
6. D.K. Galloway, M.P. Muno, J.M. Hartman, D. Psaltis, D. Chakrabarty, Thermonuclear (Type I) X-ray bursts observed by the Rossi X-ray timing explorer. Astrophys. J. Suppl. Ser. **179**, 360 (2008)
7. A. Patruno, A.L. Watts, Accreting millisecond X-ray pulsars (2020). arXiv:1206.2727 [astro-ph.HE]
8. W.B. Bonnor, The mass of a static charged sphere. Z. Phys. **160**, 59 (1960)
9. S. Ray, A.L. Espindola, M. Malheiro, J.P. Lemos, V.T. Zanchin, Electrically charged compact stars and formation of charged black holes. Phys. Rev. D **68**, 084004 (2003). arXiv:astro-ph/0307262
10. W. Sun, D. Wang, N. Xie, R.B. Zhang, X. Zhang, Gravitational collapse of spherically symmetric stars in noncommutative general relativity. Eur. Phys. J. C. **69**, 271 (2010)
11. P.M. Takisa, S. Ray, S.D. Maharaj, Charged compact objects in the linear regime. Astrophys. Space Sci. **350**, 733 (2014)
12. S.K. Maurya, Y.K. Gupta, S. Ray, S.R. Chowdhury, Spherically symmetric charged compact stars. Eur. Phys. J. C. **75**, 1 (2015)
13. J. Kumar, S.K. Maurya, A.K. Prasad, A. Banerjee, Relativistic charged spheres: compact stars, compactness and stable configurations. J. Cosmol. Astropart. Phys. **2019**, 005 (2019)
14. S.K. Maurya, S. Ray, A. Aziz, M. Khlopov, P. Chardonnet, A study on charged compact stars. Int. J. Mod. Phys. D **28**, 1950053 (2019)
15. J. Estevez-Delgado, R. Soto-Espitia, A. Cleary-Balderas, A.T. Murguía, Compact stars described by a charged model. Int. J. Mod. Phys. D **29**, 2050022 (2020)
16. M. Sharif, M.Z. Gul, Role of theory on charged compact stars. Phys. Scr. **98**, 035030 (2023)
17. B.K. Harrison, New solutions of the Einstein–Maxwell equations from old. J. Math. Phys. **9**, 1744 (1968)
18. G.W. Horndeski, Conservation of charge and the Einstein–Maxwell field equations. J. Math. Phys. **17**, 1980 (1976)
19. W. Kinnersley, Symmetries of the stationary Einstein–Maxwell field equations. II. J. Math. Phys. **18**, 1529 (1977)
20. A. Das, On the static Einstein–Maxwell field equations. J. Math. Phys. **20**, 740 (1979)
21. K. Bajer, J.K. Kowalczynski, A class of solutions of the Einstein–Maxwell equations. J. Math. Phys. **26**, 1330 (1985)
22. K. Komathiraj, S.D. Maharaj, Classes of exact Einstein–Maxwell solutions. Gen. Relativ. Gravit. **39**, 2079 (2007)
23. C. Lübbe, J.A.V. Kroon, The extended conformal Einstein field equations with matter: the Einstein–Maxwell field. J. Geom. Phys. **62**, 1548 (2012)

24. S.A. Ngubelanga, S.D. Maharaj, S. Ray, Compact stars with quadratic equation of state. Astrophys. Space Sci. **357**, 74 (2015). arXiv:1512.08994 [gr-qc]
25. B.S. Ratanpal, V.O. Thomas, D.M. Pandya, A new class of solutions of anisotropic charged distributions on pseudo-spheroidal space-time. Astrophys. Space Sci. **360**, 53 (2015). arXiv:1507.03382 [gr-qc]
26. S.A. Mardan, I. Noureen, A. Khalid, Charged anisotropic compact star core-envelope model with polytropic core and linear envelope. Eur. Phys. J. C. **81**, 912 (2021)
27. A.K. Prasad, J. Kumar, Charged Analogues of Isotropic Compact Stars Model with Buchdahl Metric in General Relativity. Astrophys. Space Sci. **366**, 1572 (2021). arXiv:1910.10471 [physics.gen-ph]
28. J. Kumar, S. Sahu, P. Bharti, A. Kumar, K. Kumar, A. Sarkar, R. Devi, Relativistic compact stars via a new class of analytical solution for charged isotropic stellar system in general relativity. Indian J. Phys. **97**, 1295 (2023)
29. A. Ditta, X. Tiecheng, A. Errehymy, G. Mustafa, S.K. Maurya, Anisotropic charged stellar models with modified Van der Waals EoS in f(Q) gravity. Eur. Phys. J. C. **83**, 254 (2023)
30. L. Rosenfeld, On the energy-momentum tensor. Mem. Acad. R. Belg. **18**, N6 (1940)
31. C.G. Callan Jr., S. Coleman, R. Jackiw, A new improved energy–momentum tensor. Ann. Phys. **59**, 42 (1970)
32. S.V. Babak, L.P. Grishchuk, Energy–momentum tensor for the gravitational field. Phys. Rev. D **61**, 024038 (1999). arXiv:gr-qc/9907027
33. D. Krupka, Variational principles for energy–momentum tensors. Rep. Math. Phys. **49**, 259 (2002)
34. R.E.G. Saravi, On the energy–momentum tensor. J. Phys. A **37**, 9573 (2004). arXiv:math-ph/0306020
35. R.I. Khrapko, The truth about the energy-momentum tensor and pseudotensor. Grav. Cosmol. **20**, 264 (2014)
36. O.M. Pimentel, F.D. Lora-Clavijo, G.A. Gonzalez, The energy–momentum tensor for a dissipative fluid in general relativity. Gen. Relativ. Gravit. **48**, 1 (2016). arXiv:1604.01318 [gr-qc]
37. R. Sharma, S. Mukherjee, Compact stars: a core-envelope model. Mod. Phys. Lett. A **17**, 2535 (2002)
38. R. Tikekar, K. Jotania, A relativistic two-parameter core-envelope model of compact stars. Grav. Cosmol. **15**, 129 (2009)
39. P.M. Takisa, S.D. Maharaj, Anisotropic charged core envelope star. Astrophys. Space Sci. **361**, 1 (2016)
40. R.P. Pant, S. Gedela, R.K. Bisht, N. Pant, Core-envelope model of super dense star with distinct equation of states. Eur. Phys. J. C **79**, 1 (2019)
41. P.M. Takisa, S.D. Maharaj, C. Mulangu, Compact relativistic star with quadratic envelope. Pramana **92**, 8 (2019)
42. S. Gedela, N. Pant, J. Upreti, R.P. Pant, Relativistic core-envelope anisotropic fluid model of super dense stars. Eur. Phys. J. C. **79**, 12 (2019)
43. A.C. Khunt, V.O. Thomas, P.C. Vinodkumar, Relativistic stellar modeling with perfect fluid core and anisotropic envelope fluid. Indian J. Phys. **97**, 3379 (2023)
44. J.S. Rowlinson, The equation of state of dense systems. Rep. Prog. Phys. **28**, 169 (1965)
45. R.J. Angel, Equations of State. Rev. Mineral. Geochem. **41**, 35 (2000)
46. S. Ray, M. Malheiro, J.P. Lemos, V.T. Zanchin, Charged polytropic compact stars. Braz. J. Phys. **34**, 310 (2004)
47. R. Sharma, S.D. Maharaj, A class of relativistic stars with a linear equation of state. Mon. Not. R. Astron. Soc. **375**, 1265 (2007)
48. S. Thirukkanesh, S.D. Maharaj, Charged anisotropic matter with a linear equation of state. Class. Quantum Gravity **25**, 235001 (2008)
49. S.A. Ngubelanga, S.D. Maharaj, Relativistic stars with polytropic equation of state. Eur. Phys. J. Plus. **130**, 1 (2015)
50. K.N. Singh, S.K. Maurya, P. Bhar, F. Rahaman, Anisotropic stars with a modified polytropic equation of state. Phys. Scr. **95**, 115301 (2020)
51. S.A. Mardan, A. Asif, I. Noureen, New classes of generalized anisotropic polytropes pertaining radiation density. Eur. Phys. J. Plus. **134**, 242 (2019)
52. S.K. Maurya, A. Banerjee, P. Channuie, Relativistic compact stars with charged anisotropic matter. Chin. Phys. C **42**, 055101 (2018)
53. Y.B. Zeldovich, The equation of state at ultrahigh densities and its relativistic limitations. J. Exp. Theor. Phys. **41**, 1609 (1961)
54. K.N. Singh, F. Rahaman, N. Pant, A well behaved charged anisotropic Tolman VII spacetime. Can. J. Phys. **94**, 953 (2016)
55. U.S. Nilsson, C. Uggla, General relativistic stars: Polytropic equations of state. Ann. Phys. **286**, 292 (2000)
56. M. Spaans, J. Silk, The polytropic equation of state of interstellar gas clouds. Astrophys. J. **538**, 115 (2000)
57. M. Azam, S.A. Mardan, I. Noureen, M.A. Rehman, Study of polytropes with generalized polytropic equation of state. Eur. Phys. J. C **76**, 1 (2016)
58. A. Nasim, M. Azam, Anisotropic charged physical models with generalized polytropic equation of state. Eur. Phys. J. C **78**, 1 (2018)
59. R. Goswami, P.S. Joshi, Gravitational collapse of an isentropic perfect fluid with a linear equation of state. Class. Quantum Gravity **21**, 3645 (2004)
60. E. Babichev, V. Dokuchaev, Y. Eroshenko, Dark energy cosmology with generalized linear equation of state. Class. Quantum Gravity **22**, 143 (2004)
61. V. Varela, F. Rahaman, S. Ray, K. Chakraborty, M. Kalam, Charged anisotropic matter with linear or nonlinear equation of state. Phys. Rev. D **82**, 044052 (2010)
62. S.A. Ngubelanga, S.D. Maharaj, S. Ray, Compact stars with linear equation of state in isotropic coordinates. Astrophys. Space Sci. **357**, 9 (2015)
63. B.V. Ivanov, Static charged perfect fluid spheres in general relativity. Phys. Rev. D **65**, 104011 (2002)
64. J. Earman, C. Glymour, The gravitational red shift as a test of general relativity: history and analysis. Stud. Hist. Philos. Sci. A **11**, 175 (1980)
65. H.A. Buchdahl, General relativistic fluid spheres. Phys. Rev. D **116**, 1027 (1959)
66. C.G. Böehmer, T. Harko, Minimum mass-radius ratio for charged gravitational objects. Gen. Relativ. Gravit. **39**, 757 (2007). arXiv:gr-qc/0702078
67. B. Dayanandan, S.K. Maurya, T.T. Smitha, Modeling of charged anisotropic compact stars in general relativity. Eur. Phys. J. A. **53**, 1434 (2017). arXiv:1611.00320 [gr-qc]
68. H. Heintzmann, W. Hillebrandt, Neutron stars with an anisotropic equation of state-mass, redshift and stability. Astron. Astrophys. **38**, 51 (1975)
69. S. Chandrasekhar, The density of white dwarf stars. Philos. Mag. **11**, 592 (1931)
70. S. Chandrasekhar, The maximum mass of ideal white dwarfs. Astrophys. J. **74**, 81 (1934)
71. S. Chandrasekhar, *An Introduction to the Study of Stellar Structure* (University of Chicago, Chicago, 1939)
72. J.R. Oppenheimer, G.M. Volkoff, On massive neutron cores. Phys. Rev. **55**, 374 (1939)
73. J.P.D. Leon, Static charged spheres with anisotropic pressure in general relativity. Gen. Relativ. Gravit. **19**, 797 (1987)
74. J.M. Lattimer, M. Prakash, Neutron star structure and the equation of state. Astrophys. J. **550**, 426 (2001)